

Dalton Transactions

Accepted Manuscript



This is an *Accepted Manuscript*, which has been through the Royal Society of Chemistry peer review process and has been accepted for publication.

Accepted Manuscripts are published online shortly after acceptance, before technical editing, formatting and proof reading. Using this free service, authors can make their results available to the community, in citable form, before we publish the edited article. We will replace this *Accepted Manuscript* with the edited and formatted *Advance Article* as soon as it is available.

You can find more information about *Accepted Manuscripts* in the [Information for Authors](#).

Please note that technical editing may introduce minor changes to the text and/or graphics, which may alter content. The journal's standard [Terms & Conditions](#) and the [Ethical guidelines](#) still apply. In no event shall the Royal Society of Chemistry be held responsible for any errors or omissions in this *Accepted Manuscript* or any consequences arising from the use of any information it contains.

ARTICLE

Catalysts of Water Oxidation and pH Sensors Based on Azo-conjugated Iridium/Rhodium Motifs

Cite this: DOI: 10.1039/x0xx00000x

Wei-Bin Yu*, Qing-Ya He, Hua-Tian Shi, Yan Pan, and Xianwen Wei*

Received 00th January 2012,
Accepted 00th January 2012

DOI: 10.1039/x0xx00000x

www.rsc.org/

Abstract. Herein we report the molecular structures and electronic properties of ionic, hydrophilic, half-sandwich complexes of the formula $[\eta^5\text{-Cp}^*\text{Ir(L)(Cl)}](\text{OTf})$ (**1**), $[\eta^5\text{-Cp}^*\text{Rh(L)(Cl)}](\text{OTf})$ (**2**), $[\eta^5\text{-Cp}^*\text{Ir(L)(H}_2\text{O)}](\text{OTf})_2$ (**3**) and $[\eta^5\text{-Cp}^*\text{Rh(L)(H}_2\text{O)}](\text{OTf})_2$ (**4**), where L is L = 1-(2-Pyridylazo)-2-naphthol. These complexes have been investigated electrochemical properties and displayed good electronic properties for using as water-oxidation catalysts. Interestingly, all of their solutions color can be transformed from brown to green at pH = 12 unambiguously, which those of **1**, **2** and **4** are especially apparent. For the reason that they can be explored as pH sensors for detecting solution pH values.

Introduction

Aromatic azo compounds are high-value chemicals widely used in industry as dyes, pigments, food additives, and drugs,¹ due to their excellent photoelectrochemical properties and tendency of degradation exposed upon UV-Vis light.² Despite these compounds are employed as electron donors for development of various transition metal complexes,³ which have exhibited different exciting properties related to electron transfer reaction, photochromism, liquid crystals, photoluminescence etc,⁴ no current complexes are utilized as catalysts for water oxidation. To our knowledge, the oxidation of water to dioxygen is carried out by green plants, algae, and cyanobacteria in order to obtain the reducing equivalents required for sustaining life processes,⁵ therefore, the exploitation of catalysts for water oxidation has attracted considerable attention.⁶ For example, manganese model systems for the water oxidation complex have been described and are most effectively driven by two-electron oxo-donating primary oxidants such as Oxone (potassium peroxydisulfate).⁷ Meanwhile, half-sandwich metal fragments have been employed for water oxidation and obtained significant results.⁸ Recently, Crabtree and co-workers

have reported mononuclear iridium water oxidation catalysts born by N-donor ligands,⁵ which exhibited highly active catalyst precursors for water oxidation.⁹ In contrast with those of naked metal utilized as catalysts' centers, the pentamethylcyclopentadienyl (Cp*) ligand utilized as a precursor of these mononuclear iridium catalysts can provide an electron rich environment, likely to stabilize the necessary high-valent intermediates required for water oxidation (Figure 1).⁵ These Cp*Ir(N-C)X and Cp*Ir(N-N)X catalysts have been displayed better activity than those reported for many other systems. On the other hand, the catalysts are mononuclear, are easy to make, and continue to catalyze oxygen evolution over hours.⁵

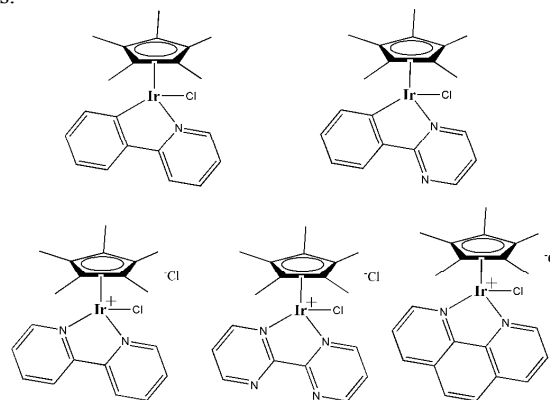


Figure 1. Iridium(III) catalysts for water oxidation reported by Crabtree and co-worker.

Since these iridium catalysts were available for water oxidation, we decided to synthesize novel half-sandwich iridium and rhodium fragments bound by aromatic azo compounds, because of not only excellent electrochemical properties of azo compounds,¹⁰ but also successful construction

Analysis and Testing Central Facility, School of Chemistry and Chemical Engineering, Anhui University of Technology, Maanshan 243002, P.R.China. E-mail: yuweibin@ahut.edu.cn; xwwei@ahut.edu.cn.

Fax: +86 555 2471263; Tel: +86 555 2311087

Electronic Supplementary Information (ESI) available: ¹H/¹³C/¹⁹F NMR, UV-vis spectra and CV curves, crystal data and Crystallographic information files of complexes 2-4. This material is available free of charge via the Internet at <http://pubs.rsc.org>.

of half-sandwich iridium frameworks reported in previous works.¹¹

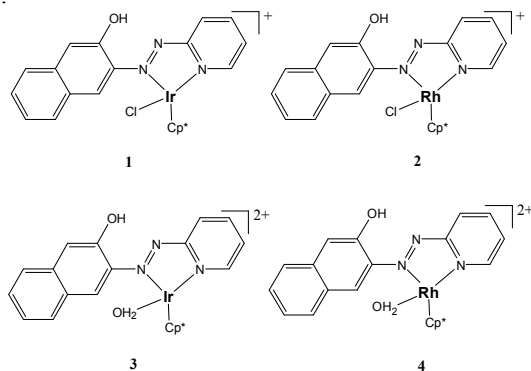


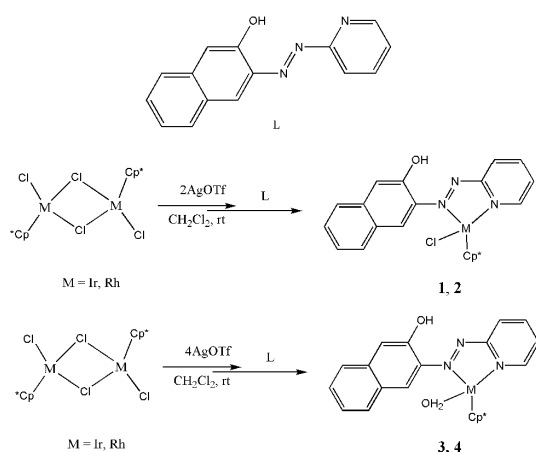
Figure 2. Iridium(III) and rhodium(III) catalysts for water oxidation.

We now report full details on complexes $[\eta^5\text{-Cp}^*\text{Ir(L)(Cl)}](\text{OTf})$ (**1**) a $[\eta^5\text{-Cp}^*\text{Rh(L)(Cl)}](\text{OTf})$ (**2**), and also compare their behavior with related complexes $[\eta^5\text{-Cp}^*\text{Ir(L)(H}_2\text{O)}](\text{OTf})_2$ (**3**) and $[\eta^5\text{-Cp}^*\text{Rh(L)(H}_2\text{O)}](\text{OTf})_2$ (**4**) (Figure 2).

Results and Discussion

Syntheses of azo-conjugated complexes **1-4**. The syntheses of $[\text{Cp}^*\text{IrCl}_2]_2$ and $[\text{Cp}^*\text{RhCl}_2]_2$ have been well-established,¹² and this azo-ligand (L = 1-(2-Pyridylazo)-2'-naphthol) has been purchased from TCI (Shanghai) co., LTD. The most versatile and general method of preparing half-sandwich Ir/Rh organometallic complexes are a reaction involving a removal halide of metal. Herein, we employ the one-pot method of synthesizing these azo-conjugated organometallic complexes **1-4** as described in Scheme 1.

Mononuclear complexes $[\text{Cp}^*\text{IrLCl}](\text{OTf})$ (**1**) and $[\text{Cp}^*\text{RhLCl}](\text{OTf})$ (**2**) are readily formed upon removal of two Cl⁻ ions from $[\text{Cp}^*\text{IrCl}_2]_2$ and $[\text{Cp}^*\text{RhCl}_2]_2$ treated by 2 equiv of AgOTf (silver triflate), respectively. Meanwhile, $[\text{Cp}^*\text{IrL(H}_2\text{O)}](\text{OTf})_2$ (**3**) and $[\text{Cp}^*\text{RhL(H}_2\text{O)}](\text{OTf})_2$ (**4**) are obtained by reacting $[\text{Cp}^*\text{IrCl}_2]_2$ and $[\text{Cp}^*\text{RhCl}_2]_2$ with 4 equiv of AgOTf, respectively. The products are obtained as brown powders in good yields and excellent purity. Complexes **1-4** are highly soluble in alcohols and moderately soluble in donor solvents such as water. All were characterized by elemental analysis, ESI-MS, ¹H NMR, ¹³C NMR, ¹⁹F NMR and IR spectroscopy.



Scheme 1. Synthetic processes of complexes **1-4**.

The ¹H NMR spectrum of **1** suggests that the Cp* groups were split into two parts ratio of 1:4, indicating different chemical environments of the -OH group. The existence of isomers is probably due to the different configuration of the phenyl groups (Figure 3). The spectra of complexes **2** and **4** reveal that the Cp* groups were split into two parts similar to those of complex **1** in methanol solution (see the Supplementary information). Interestingly, the ¹H NMR spectra of **3** do not discover the same phenomenon (Figure 4) as those of **1-3**. These ¹H NMR spectra have demonstrated that the frameworks of complexes **1-4** are identical. ESI-MS are carried out to further confirm their main skeletons, proving the proof for demonstrations of NMR spectra (see the Supplementary information).

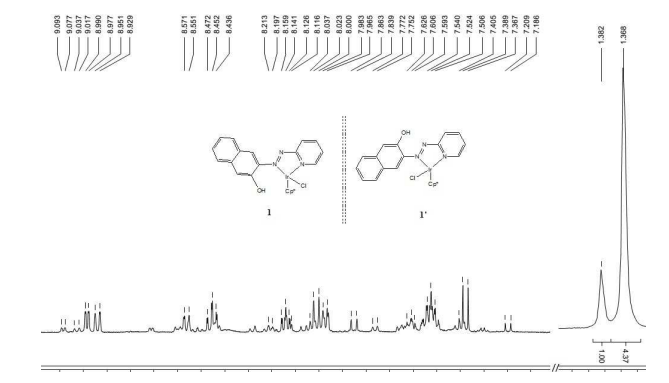


Figure 3. Top: two proposed structures of isomers of **1**; bottom: ¹H NMR spectrum of **1** in CD₃OD.

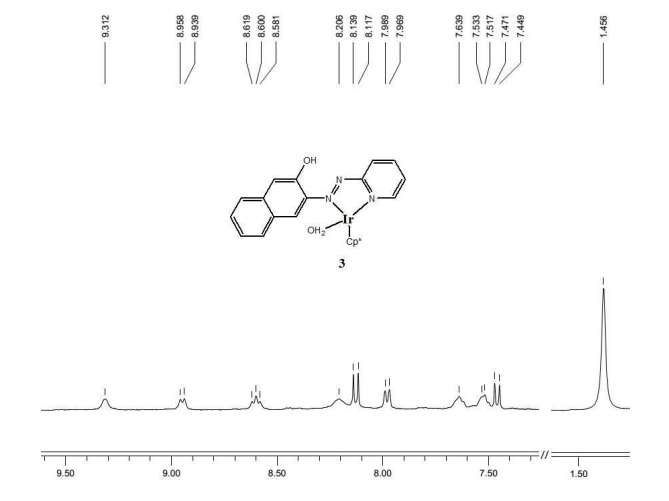


Figure 4. Top: the structure of **3**; bottom: ¹H NMR spectrum of **3** in CD₃OD.

The suitable crystals of **2-4** for single-crystal X-ray diffraction to confirm their own structures were obtained by diffusion of ether into complexes **2-4** methanol solution for several days. Their structures of **2-4** reveal their structures were consistent with that of those characterizations by ¹H NMR and MS.

The analysis of these X-ray data confirms the conclusions that have been drawn from 1D NMR data with regard to the configuration of N=N groups. We note that azo ligand L keep

trans symmetric geometry in complexes **2-4**, which linked to the half-sandwich metal atom to construct five-member ring metallacycles. This configuration occupied the centers of Ir/Rh atoms on one side and the other side of that for solvent molecules coordination, which supplies space for water oxidation to take place.

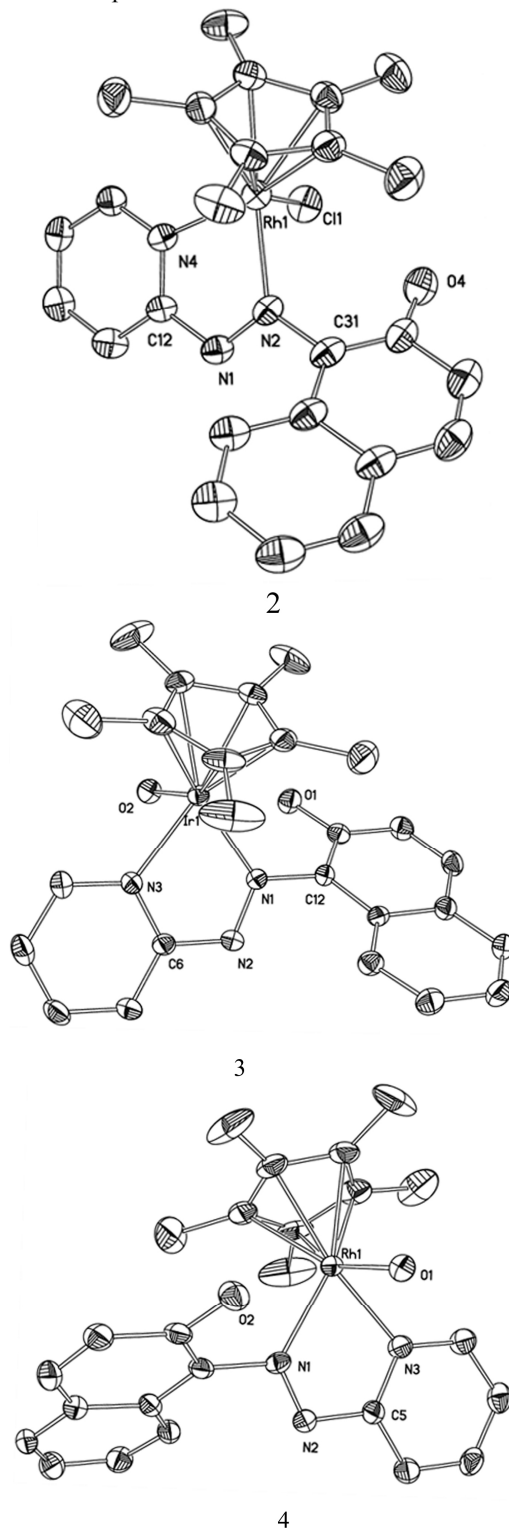


Figure 5. ORTEP drawing of complexes **2-4** (30% thermal ellipsoids). H atoms and OTf are omitted for clarity. Selected

bonds (Å) and angles (°). Rh(1)-N(4) = 2.087(6), Rh(1)-N(2) = 2.093(6), Rh(1)-Cl(1) = 2.409(2); N(4)-Rh(1)-N(2) = 75.1(2), N(4)-Rh(1)-Cl(1) = 84.55(16), N(2)-Rh(1)-Cl(1) = 87.81(16) for **2**. Ir(1)-N(1) = 2.085(5), Ir(1)-N(3) = 2.097(5), Ir(1)-O(2) = 2.170(4); N(1)-Ir(1)-N(3) = 74.62(2), N(1)-Ir(1)-O(2) = 91.36(2), N(3)-Ir(1)-O(2) = 81.72(2) for **3**. Rh(1)-N(3) = 2.102(9), Rh(1)-N(1) = 2.106(9), Rh(1)-O(1) = 2.178(8); N(3)-Rh(1)-N(1) = 73.8(3), N(3)-Rh(1)-O(1) = 82.3(4), N(1)-Rh(1)-O(1) = 92.6(3) for **4**.

Spectrochemistry. Spectrochemical experimental were performed on complexes **1-4** in water solvent in order to evaluate the effects of the metal cation and coordination mode on the electronic structures. As exemplified in Figure 6, the electronic spectra of the compounds display a broad absorption band in the visible region (554 nm for **1**, 542 nm for **2**, 552 nm for **3** and 540 nm for **4**, respectively) as a common feature. In contrast, the λ_{\max} values of a $\pi-\pi^*$ transition band ascribe to the azo moiety in the trans form of this ligand L was at 482 nm as reported,¹³ suggesting the complexes **1-4** giving strong bands between L and metal in this region. The bands are significantly shifting a lower energy for **1-4**. The electronic spectra of closed complexes **1-4**, however, are significantly different from those of them in terms of the separation $n-\pi^*$ bands their respective λ_{\max} values (Figure 6), because the UV-Vis spectra of **1-4** display double low-intensity $n-\pi^*$ bands in the 350-450 nm region. As Figure 6 shown, it suggests that the **1-4** does not alter the electronic structure in different solvent. Additionally, these complexes in organic solvent like methanol exhibit red-shift tendency (see the Supplementary information).

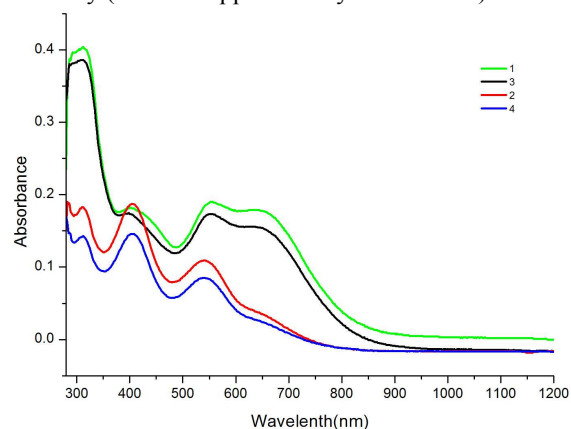
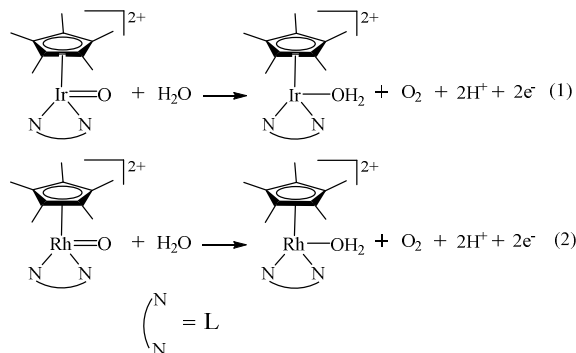


Figure 6. UV-Vis spectra of **1-4** in water.

Electrochemistry. Cyclic voltammograms were measured for complexes **1-4** in water PBS (Phosphate Buffered Saline) utilized as assistant electrolyte at room temperature with 50 mV/s scan rate. Electrochemistry allows us to examine the oxidation behavior of these complexes over a much wider pH range. Complexes **1-4** are soluble in aqueous solutions in the Ir(III) and Rh(III) oxidation state, allowing us to examine electrochemically driven oxidations in aqueous solution. A schematic version of the proposed pathway is given in eq 1 and 2.⁵



In the light of the eq. 1 and 2, the central metals with a reversible or quasi-reversible redox reaction, we speculate the effects of potentials in complexes **1** and **2** based on their Nerst equations 3 and 4.

$$E = E_0 - \frac{RT}{2F} \ln \frac{a_{\text{Ir}^{3+}} a_{\text{O}_2} a_{\text{H}^+}^2}{a_{\text{Ir}^{5+}}} \quad (3)$$

$$E = E_0 - \frac{RT}{2F} \ln \frac{a_{\text{Rh}^{3+}} a_{\text{O}_2} a_{\text{H}^+}^2}{a_{\text{Rh}^{5+}}} \quad (4)$$

Where E_0 represents the reduction potential for the aqueous Ir(V/III) and Rh(V/III) couple expressed in terms of concentrations, and a represents the activity. From the two equations, we observed that E value of complexes **1-4** tested by CV were influenced by the concentration of the Ir and Rh fragment solutions and their pH values. Therefore, when controlling their concentration and pH values, different E were obtained by CV coinciding with our experimental (Table 1 and 2).

Compound	[C] (mM)	CV peaks ([Red]/[Oxi](V))
1	0.01	-0.843, -0.469/0.361, -0.297
1	0.02	-0.835, -0.465/0.393, -0.334
1	0.03	-0.486/0.393
1	0.04	-0.490/0.399
1	0.05	-0.486/-0.285
2	0.01	-0.486/-0.364
2	0.02	-0.477/-0.347
2	0.03	-0.402/-0.087
2	0.04	-0.482/-0.326
2	0.05	-0.490/-0.343
3	0.01	-0.809/-0.427
3	0.02	-0.541/-0.364
3	0.03	-0.351/-0.045
3	0.04	-0.578/-0.515
3	0.05	-0.557/-0.498
4	0.01	-0.431/-0.334
4	0.02	-0.469/-0.343
4	0.03	-0.453/-0.039
4	0.04	-0.482/-0.347
4	0.05	-0.528/-0.406

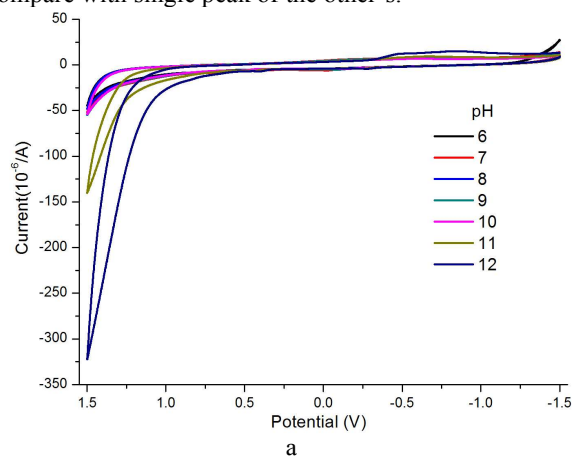
Table.1 CV peaks of pH-dependent cyclic voltammograms of compounds **1-4**. (Concentration = 0.03 mM)

Compounds	pH	CV peaks ([Red]/[Oxi](V))
-----------	----	---------------------------

1	6	0.742, -0.026 [Oxi]
1	7	0.651, -0.037 [Oxi]
1	8	0.640, -0.074 [Oxi]
1	9	0.577, -0.096 [Oxi]
1	10	0.526, -0.137 [Oxi]
1	11	0.419, -0.217 [Oxi]
1	12	0.390, -0.280 [Oxi]
2	6	-0.305/-0.020
2	7	-0.317/-0.028
2	8	-0.402/-0.087
2	9	-0.410/-0.099
2	10	-0.442/-0.196
2	11	-0.544/0.731
2	12	-0.515/0.693
3	6	-0.300/-0.085
3	7	-0.385/-0.003
3	8	-0.351/-0.045
3	9	-0.335/-0.087
3	10	-0.436/-0.142
3	11	-0.556/-0.238
3	12	-0.623[Red]
4	6	-0.238/-0.066
4	7	-0.283/-0.096
4	8	-0.453/-0.039
4	9	-0.515/-0.141
4	10	-0.453/-0.200
4	11	-0.566/-0.280
4	12	-0.612/-0.343

Table.2 CV peaks of concentration-dependent cyclic voltammograms of compounds **1-4**. (pH = 12)

As Table 1 and 2 displayed, all complexes in aqua solutions took place redox reaction reversibly or quasi-reversibly, therefore, all of these were in accordance with Nerst Eq. 3 and 4. However, there are apparent difference from complex **1** and the other, the former show double oxidation peaks in CV curves to compare with single peak of the other's.



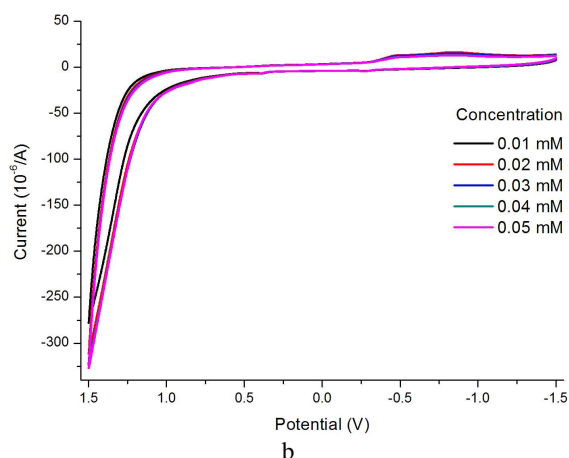


Figure 7. a) pH-dependent cyclic voltammograms of complex **1** in aqueous solution (Concentration: 0.03 mM, scan rate: 50 mV/s); b) Concentration-dependent cyclic voltammograms of complex **1** in aqueous solution (pH = 12, scan rate: 50 mV/s).

Cyclic voltammograms collected for complex **1** at various pH values and concentration are shown in Figure 7. Visibly, these CV peaks turn up different status under different pH values and concentration, in complete according to Nernst equation and previous works.⁵ In addition, as Figure 7a demonstrated, A prominent catalytic wave at ca. pH = 12 appeared. On the other hand, prominent CV peaks of the other complexes **2-4** are similar to that of **1**, due to them emerging at pH = 12 (0.70 V for **2**, 0.78 V for **3** and 0.73 V for **4**, respectively), suggesting complexes **1-4** similarity of electrochemical properties (see the Supplementary information).

A plausible reaction mechanism for Ir/Rh-catalyzed water oxidation, taking into account the mononuclear nature of our catalysts, is shown in Figure 8. With a neutral chloro catalyst or with a ionic catalyst, such as **1** or **2** and **3** or **4**, the Cl⁻ ion is replaced by a molecule of H₂O yielding a cationic Ir(III)/Rh(III) aqua complex. This intermediate is oxidized by cerium(IV) to an Ir(III) or Rh(III) oxo complex, which acts as active species in the formation of the O-O bond by reacting with water. The oxidation of the resulting peroxo intermediate yields the final O₂ product, and the catalyst is recovered by coordination of H₂O.⁵

Interestingly, during investigating electrochemical properties of complexes **1-4** at various pH values, we have observed that the transformation of color from brown to green in these aqua solution when pH values are 12 (see the Supplementary information). Characterization of their solution at pH = 12 by ESI-MS has proved that their main frameworks are not decomposed (see the Supplementary information). It is worthing notice that the complexes can be employed as sensors of solution at various pH values based on the transformation.¹⁴

Experimental Section

General. All solvents were of commercial grade and dried over activated alumina using a Grubbs-type solvent purification system prior to use.¹⁵ ¹H, ¹³C and ¹⁹F NMR spectra were collected on a 400 MHz Bruker spectrometer. UV-Vis spectra were collected using a Varian Cary 50 Bio UV-Vis spectrometer with samples in a 1.0 cm quartz cuvette at pH 7.0. The starting materials [Cp*IrCl(μ-Cl)]₂ and [Cp*RhCl(μ-Cl)]₂ were prepared according to the literature methods.¹² Elemental analyses were performed on an Elementar III Vario EI analyzer.

IR spectra are measured on a Nicolet Avatar-360 spectrophotometer (as KBr pellet).

Syntheses of [η⁵-Cp*Ir(L)(Cl)](OTf) (**1**) and [η⁵-Cp*Rh(L)(Cl)](OTf) (**2**)

[Cp*IrCl₂]₂ (80.0 mg, 0.1 mmol) and [Cp*RhCl₂]₂ (62.0 mg, 0.1 mmol) were dissolved in 8 mL of CH₂Cl₂ at room temperature. To these solutions were added 2 equiv of AgOTf (51.2 mg, 0.2 mmol) sheltered from light. After stirring 6.0 h at room temperature, the reaction solution was added to about 2.0 mmol (50.0 mg) of ligand (L = 1-(2-Pyridylazo)-2-naphthol) and kept vigorously stirring for 6 hours, brown precipitate collected by vacuum filtration in air. **1**, Yield, 108.1 mg, 71%. **2**, Yield, 104.8 mg, 78%.

Complex 1: Anal. Calcd for C₂₆H₂₆ClF₃IrN₃O₄S: C, 41.02; H, 3.44; N, 5.52. Found: C, 40.97; H, 3.41; N, 5.49. ¹H NMR (400 MHz, methanol-*d*₄) δ (ppm): 1.36 (d, 15H, Cp*), 9.10-7.19 (m, aromatic groups); ¹³C NMR(100.6 MHz, methanol-*d*₄) δ (ppm): 6.92, 89.75 (Cp*), 95.38, 117.29, 118.15, 119.58, 122.00, 122.82, 124.68, 125.59, 126.06, 127.30, 127.82, 128.00, 128.17, 128.24, 128.58, 128.81, 129.63, 130.19, 130.33, 133.06, 142.75, 146.61, 150.60, 165.80 (aromatic groups). ¹⁹F NMR(376.5 MHz, methanol-*d*₄) δ(ppm): -80.14, -80.13. ESI-MS (MS, ES⁺) m/z, calcd for [η⁵-Cp*Ir(L)]²⁺: 577.17; Found: 577.00. IR (KBr pellet), cm⁻¹: 3423.5 (m), 3137.3 (m), 3071.0 (m), 1627.7 (m), 1594.5 (w), 1565.4 (w), 1441.0 (w), 1289.8 (s), 1236.3 (s), 1217.7 (s), 1163.1 (s), 1027.5 (s), 972.4 (w), 835.5 (w), 780.0 (w), 756.7 (w).

Complex 2: Anal. Calcd for C₂₆H₂₆ClF₃RhN₃O₄S: C, 46.48; H, 3.90; N, 6.25. Found: C, 46.43; H, 3.88; N, 6.21. ¹H NMR (400 MHz, methanol-*d*₄) δ (ppm): 1.45 (d, 15H, Cp*), 7.22-9.35 (m, aromatic groups); ¹³C NMR(100.6 MHz, methanol-*d*₄) δ (ppm): 7.39, 95.30(Cp*), 98.29, 98.37, 100.03, 100.09, 112.34, 117.65, 118.81, 119.55, 121.88, 121.97, 123.35, 125.05, 128.12, 128.63, 129.40, 129.65, 129.83, 130.23, 133.93, 143.83, 144.22, 151.36 (aromatic groups). ¹⁹F NMR(376.5 MHz, methanol-*d*₄) δ(ppm): -80.74, -80.59. ESI-MS (MS, ES⁺) m/z, calcd for [η⁵-Cp*Rh(L)]²⁺: 487.11; Found: 486.00. IR (KBr pellet), cm⁻¹: 3442.2 (m), 3187.1 (m), 3104.2 (m), 1623.5 (m), 1610.0 (m), 1536.4 (m), 1507.4 (m), 1461.8 (w), 1395.4 (w), 1289.7 (s), 1248.6 (s), 1224.3 (s), 1171.6 (s), 1151.7 (s), 1088.5 (w), 1025.0 (s), 839.6 (w), 765.0 (w), 740.1 (w), 636.9 (w).

Syntheses of [η⁵-Cp*Ir(L)(H₂O)](OTf)₂ (**3**) and [η⁵-Cp*Rh(L)(H₂O)](OTf)₂ (**4**)

[Cp*IrCl₂]₂ (80.0 mg, 0.1 mmol) and [Cp*RhCl₂]₂ (62.0 mg, 0.1 mmol) were dissolved in 8 mL of CH₂Cl₂ at room temperature. To these solutions were added 4 equiv of AgOTf (102.4 mg, 0.4 mmol) sheltered from light. After stirring 12.0 h at room temperature, the reaction solution was added to about 2.0 mmol (50.0 mg) of ligand L and kept vigorously stirring overnight, brown precipitate collected by vacuum filtration in air. **3**, Yield, 142.9 mg, 80%. **4**, Yield, 130.2 mg, 81%.

Complex 3: Anal. Calcd for C₂₇H₂₈F₆N₃O₈IrS₂: C, 36.32; H, 3.16; N, 4.71. Found: C, 36.33; H, 3.13; N, 4.68. ¹H NMR (400 MHz, methanol-*d*₄) δ (ppm): 1.46 (s, 15H, Cp*), 7.44-9.31 (aromatic group). ¹³C NMR(100.6 MHz, methanol-*d*₄) δ (ppm): 7.33, 88.79 (Cp*), 93.57, 95.45, 109.53, 112.36, 113.47,

117.65, 118.82, 120.46, 121.99, 123.49, 125.15, 125.22, 127.25, 127.30, 127.96, 128.02, 128.29, 128.58, 129.31, 129.70, 130.09, 134.29, 135.05, 144.23, 147.46, 148.92, 151.04 (aromatic group). ^{19}F NMR(376.5 MHz, methanol- d_4) δ (ppm): -79.98, -79.96. ESI-MS (MS, ES^+) m/z , calcd for $[\eta^5\text{-Cp}^*\text{Ir(L)}]^{2+}$: 577.17; Found: 577.00. IR (KBr pellet), cm^{-1} : 3440.1 (m), 3184.5 (m), 1627.7 (w), 1606.9 (w), 1569.6 (w), 1515.7 (w), 1441.0 (w), 1374.7 (w), 1287.9 (s), 1238.1 (s), 1224.7 (s), 1177.8 (s), 1161.1 (s), 1029.8 (s), 922.6 (w), 860.4 (w), 831.3 (w), 773.3 (w).

Complex 4: Anal. Calcd for $\text{C}_{27}\text{H}_{28}\text{F}_6\text{N}_3\text{O}_8\text{RhS}_2$: C, 40.36; H, 3.51; N, 5.23. Found: C, 40.40; H, 3.48; N, 5.22. ^1H NMR (400 MHz, methanol- d_4) δ (ppm): 1.45 (d, 15H, Cp*), 7.22-9.47 (m, aromatic groups). ^{13}C NMR(100.6 MHz, methanol- d_4) δ (ppm): 7.41 (d), 95.35 (d) (Cp*), 100.00, 100.10, 112.34, 113.46, 117.59, 118.80, 120.67, 121.97, 123.32, 125.08, 125.46, 128.44, 128.59, 128.76, 129.42, 131.49, 135.05, 137.39, 143.83, 144.22, 151.34, 163.10 (aromatic groups). ^{19}F NMR(376.5 MHz, methanol- d_4) δ (ppm): -80.03, -80.02. ESI-MS (MS, ES^+) m/z , calcd for $[\eta^5\text{-Cp}^*\text{Rh(L)}]^{2+}$: 487.11; Found: 486.00. IR (KBr pellet), cm^{-1} : 3443.2 (m), 3195.1 (m), 1623.5 (w), 1598.6 (w), 1573.7 (w), 1515.7 (w), 1287.3 (s), 1239.3 (s), 1224.8 (s), 1212.7 (s), 1176.8 (s), 1159.9 (s), 1030.6 (s), 914.3 (w), 860.4 (w), 827.2 (w), 789.9 (w), 756.7 (w).

X-ray crystal structure determinations

All single crystals were immersed in mother solution and sealed in thin-walled glass. Data were collected on a CCD-Bruker SMART APEX system. All the determinations of unit cell and intensity data were performed with graphite-monochromated $\text{MoK}\alpha$ radiation ($\lambda = 0.71073 \text{ \AA}$). All the data were collected at room temperature using the ω scan technique. These structures were solved by direct methods, using Fourier techniques, and refined on F2 by a full-matrix least-squares method. All the calculations were carried out with the SHELXTL program.¹⁶ A summary of the crystallographic data and selected experimental information are given in supporting information.

Crystallographic data (excluding structure factors) for the structure analysis have been deposited with the Cambridge Crystallographic Data Centre, CCDC No. 979114 (2), No. 979115 (3), and 979116 (4). Copies of this information may be obtained free of charge on application to the Director, CCDC, 12 Union Road, Cambridge, CB21EZ, UK (fax: +44 1223 336033; e-mail: deposit@ccdc.cam.ac.uk or www: http://www.ccdc.cam.ac.uk).

Conclusions

Half-sandwich “piano-stool” complexes $[\eta^5\text{-Cp}^*\text{Ir(L)(Cl)}](\text{OTf})$ (1), $[\eta^5\text{-Cp}^*\text{Rh(L)(Cl)}](\text{OTf})$ (2), $[\eta^5\text{-Cp}^*\text{Ir(L)(H}_2\text{O)}](\text{OTf})_2$ (3) and $[\eta^5\text{-Cp}^*\text{Rh(L)(H}_2\text{O)}](\text{OTf})_2$ (4) have been synthesized and characterized by NMR, EA, MS and X-ray crystallography. The complexes are the first examples of half-sandwich complexes of iridium and rhodium with (N, N) azo-dye ligand explored for oxidation of water and displayed interesting photochemistry. Aqueous electrochemical studies on the complexes show a catalytic oxidation wave at a potential of 0.70-0.90 V at pH = 12.0. Electronic photochemical studies show that different half-sandwich metal moieties coordinated by azo-dye ligand (L) have great effect on the $n\text{-}\pi^*$ bands but little effect on $\pi\text{-}\pi^*$ transition bands in complexes 1-4. Surprisingly, when the pH values of solution is 12, their

solution color are transformed from brown to green, which can be explored as pH sensors for detecting pH values of aqua solutions.

Acknowledgements

This work was supported by the National Science Foundation of China (21301003, 21271006).

Notes and references

- (a) R. Egli, in *Colour Chemistry: The Design and Synthesis of Organic Dyes and Pigments*, (Eds: A. P. Peter, H. S. Freeman), Elsevier, London, 1991, chap. VII. (b) S. C. Catino, E. Farris, *Concise Encyclopedia of Chemical Technology*, Wiley, New York, 1985. (c) K. Venkataraman, in *The Chemistry of Synthetic Dyes*, Academic Press, London, 1970, chap. VI.
- (a) F. Zhang, Y. J. Liu, Q. H. Liu, Q. Li, H. Li, X. Y. Cai, and Y. D. Wang, *Mater. Technol.* 2013, **28**, 310-315. (b) Y. J. Wang, H. Y. Zhao, J. X. Gao, G. H. Zhao, Y. G. Zhang, and Y. L. Zhang, *J. Phys. Chem. C* 2012, **116**, 7457-7463. (c) F. Jamal, T. Qidwai, P. K. Pandey, R. Singh, and S. Singh, *Catal. Commun.* 2011, **12**, 1218-1223.
- (a) H. Zollinger, *Color Chemistry: Syntheses, Properties and Application of Organic Dyes and Pigments, second ed.*, VCH, Weinheim, 1991. (b) S. Kawata, and Y. Kawata, *Chem. Rev.* 2000, **100**, 1777-1788. (c) J. A. Delaire, and K. Nakatani, *Chem. Rev.* 2000, **100**, 1817-1845. (d) G. Pavlovic, L. Racane, H. Cicak, V. Tralic-Kulenovic, *Dyes Pigments* 2009, **83**, 354-362.
- (a) B. K. Ghosh, and A. Chakravorty, *Coord. Chem. Rev.* 1989, **95**, 239-266. (b) A. C. G. Hotze, H. Kooijman, A. L. Spek, J. G. Haasnoot, and J. Reedijk, *New J. Chem.* 2004, **28**, 565-569. (c) B. K. Santra, and G. K. Lahiri, *J. Chem. Soc. Dalton Trans.* 1998, 1613-1618. (d) G. K. Lahiri, S. Bhattacharya, S. Goswami, and A. Chakravorty, *J. Chem. Soc. Dalton Trans.* 1990, 561-565. (e) P. Byabartta, J. Dhinda, P. K. Santra, C. Sinha, K. Panneerselvam, F. -L. Liao, and T. -H. Lu, *J. Chem. Soc. Dalton Trans.* 2001, 2825-2832. (f) K. K. Sarker, B. G. Chand, K. Suwa, J. Cheng, T. -H. Lu, J. Otsuki, and C. Sinha, *Inorg. Chem.* 2007, **46**, 670-680.
- (a) J. D. Blakemore, N. D. Schley, D. Balcells, J. F. Hull, G. W. Olack, C. D. Incarvito, O. Eisenstein, G. W. Brudvig, and R. H. Crabtree, *J. Am. Chem. Soc.* 2010, **132**, 16017-16029. (b) W. -B. Yu, Q. -Y. He, H. -T. Shi, J. -Y. Jia, and X. Wei, *Dalton Trans.* 2014, DOI: 10.1039/C4DT00055B.
- (a) J. P. McEvoy, G. W. Brudvig, *Chem. Rev.* 2006, **106**, 4455-4483. (b) H. Dau, C. Limberg, T. Reier, M. Risch, S. Roggan, and P. Strasser, *ChemCatChem* 2010, **2**, 724-761.
- (a) J. Limburg, J. S. Vrettos, L. M. Liable-Sands, A. L. Rheingold, R. H. Crabtree, and G. W. Brudvig, *Science* 1999, **283**, 1524-1527. (b) P. Kurz, G. Berggren, M. F. Anderlund, and S. Styring, *Dalton Trans.* 2007, 4258-4261.
- N. D. McDaniel, F. J. Coughlin, L. L. Tinker, and S. Bernhard, *J. Am. Chem. Soc.* 2008, **130**, 210-217.
- J. F. Hull, D. Balcells, J. D. Blakemore, C. D. Incarvito, O. Eisenstein, G. W. Brudvig, and R. H. Crabtree, *J. Am. Chem. Soc.* 2009, **131**, 8730-8731.

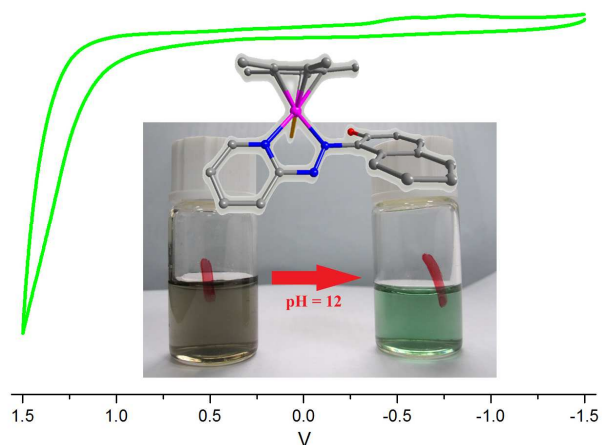
- 10 (a)A. Das, T. M.Scherer, S. M.Mobin, and W. Kaim, *Chem. Eur. J.* 2012, **18**, 11007-11018. (b)S. Joy, P. Pal, T. K. Mondal, G. B. Talapatra, and S. Goswami, *Chem. Eur. J.* 2012, **18**, 1761-1771.
- 11 (a)T. Wu, Y. -J. Lin, and G. -X. Jin, *Dalton Trans.* 2013,**42**, 82-88. (b)T. Wu, L.-H. Weng, and Guo-Xin Jin, *Chem. Comm.* 2012, **48**, 4435-4437.(c)Y. -F. Han, Y.-B. Huang, Y. -J. Lin, and G. -X. Jin, *Organometallics*, 2008, **27**, 961-966. (d) Y. -F. Han, H. Li, P. Hu, and G. -X. Jin, *Organometallics*, 2011, **30**, 905-911.(e)Y. -F. Han, H. Li, G. -X. Jin. *Chem. Commun.*, 2010, **46**, 6879-6890. (f)Y. -F. Han, G. -X. Jin, *Chem. Asian J.*, 2011, 6, 1348-1352.(g)Y. -F. Han, G. -X. Jin, *Chem. Soc. Rev.* 2014, DOI: 10.1039/c3cs60343a. (h) S. -L. Huang, Y. -J. Lin, T. S. Andy Hor, and G.-X. Jin, *J. Am. Chem. Soc.*, 2013, **135**, 8125-8128. (i)Z. -J. Yao, W. -B. Yu, Y.-J. Lin, S. -L. Huang, Z. -H. Li, and G. -X. Jin, *J. Am. Chem. Soc.*, 2014, **136**, 2825-2832.(j)H. Li, Y. -F. Han, Y. -J. Lin, Z. -W. Guo, and G. -X. Jin, *J. Am. Chem. Soc.*, 2014, **136**, 2982-2985.(k) Y.-F. Han, Y. -J. Lin, L. -H. Weng, H. Berke, and G. -X. Jin, *Chem. Commun.*, 2008, 350-352.(l)Y. -F. Han, Y. -J. Lin, and G. -X. Jin, *Dalton Trans.*, 2011, **40**, 10370-10375.(m) Y. -F. Han, W. -G. Jia, Y. -J. Lin, and G. -X. Jin, *Angew. Chem. Int. Ed.*, 2009, **48**, 6234-6238. (n) Y.-F. Han, Y. Fei, and G.-X. Jin, *Dalton Trans.*, 2010, **39**, 3976-3984.
- 12 C. White, A. Yates, and P. M. Maitles, *Inorg. Synth.* 1992, **29**, 228-234.
- 13 (a)M. Nihei, M. Kurihara, J. Mizutani, and H. Nishihara, *J. Am. Chem. Soc.* 2003, 125, 2964-2973. (b)H. Rau, *Angew. Chem. Int. Ed.* 1973, **12**, 224-235.
- 14 (a)D. Escudero, S. Trupp, B. Bussemer, G. J. Mohr, and L. Gonzalez, *J. Chem. Theory. Comput.* 2011, **7**, 1062-1072. (b)A. M. Costero, M. Parra, S. Gil, R. Martinez-Manez, F. Sancenon, and S. Royo, *Chem-Asian J.* 2010, **5**, 1573-1585.
- 15 A. B. Pangborn, M. A. Giardello, R. H. Grubbs, R. K. Rosen, and F. J. Timmers, *Organometallics* 1996, **15**, 1518-1520.
- 16 G. M. Sheldrick, *SHELXL-97*; Universität Göttingen: Germany, 1997.

For Table of Contents entry only

Catalysts of Water Oxidation and pH Sensors Based on Azo-conjugated Iridium/Rhodium Motifs

Wei-Bin Yu*, Qing-Ya He, Hua-Tian Shi, Yan Pan, and Xianwen Wei*

Analysis and Testing Central Facility, School of Chemistry and Chemical Engineering, Anhui University of Technology, Maanshan 243002, P.R.China.



Ionic half-sandwich Ir(III) and Rh(III) fragments coordinated by azo compounds exhibit good electrochemical properties, that is, they can be employed utilized as catalyst for water oxidation. Interestingly, the transformation of these complexes solutions' color from brown to green occurs at 12 of their aqua solutions pH values, which can be utilized as pH sensors.